A Comparison of Different Wireless LAN Transmission Techniques Using Ray Tracing

Aram Falsafi*, Kaveh Pahlavan*, Ganing Yang**
*Center for Wireless Information Network Studies, WPI, Worcester, MA
** Rockwell Telecommunications, Newport Beach, CA

Abstract

This paper presents a comparison among the performances of various transmission technologies in a typical indoor radio environment. The performance of frequency hopping and direct sequence spread spectrum are compared with the performance of multicarrier, decision feedback equalizer, and sectored antenna systems. Given a maximum tolerable outage probability, the maximum achievable data rates are obtained for the different modulation techniques. Outage probabilities are estimated through simulation, using channel impulse responses obtained from ray tracing. The bandwidth efficiency of spread spectrum modulation is shown be very low. For a fixed bandwidth, the minimum power requirement of each modulation technique is also presented, showing significantly lower power requirements for spread spectrum. Overall, multicarrier modulation is found to present the best tradeoff between bandwidth efficiency and power consumption.

1. Introduction

In the US, the Industrial, Scientific, Medical (ISM) bands were released in May 1985 as unregulated secondary bands for wireless data communications using spread spectrum modulation. The IEEE 802.11 committee was formed in 1990. Its goal is to develop interoperability standards for wireless networks that use either spread spectrum modulation in the 2.4 GHz ISM band or diffused infrared (DFIR) transmission [IEEE94]. In 1993, the EC announced allocations in the 5.2 and 17.1 GHz bands for the development of HIPERLAN networks. RES 10 is chartered to define a radio transmission technique that includes type of modulation, coding, channel access, and MAC-layer protocols [Bou94]. The physical-layer transmission techniques considered for the two standards are quite different. This situation has created the need for a quantitative study of the performance of different transmission techniques in a typical indoor environment.

Given an estimate of the channel impulse response, it is possible to predict the performance of different modulation schemes in that channel. Three methods have been used for generating channel impulse responses; statistical channel modeling, direct measurements, and ray tracing. Earlier performance evaluation studies such as [Kav87] have used statistical channel models and estimated the performance of different systems using either derivations or Monte-Carlo simulations. Realizing the need for more accurate *site-specific* propagation estimates, other researchers have directly used the results of wideband measurements, as their channel impulse responses [Cha93]. However, wideband measurements at every site of interestare not cost-effective. Ray tracing has been proposed as a more economical method of predicting the propagation of radio waves in indoor, metropolitan, and rural areas -- it requires only the floorplan of the site and a high-performance general purpose computer [Yan94b]. Ray tracing also provides direction-of-arrival information, which is necessary for analyzing sectored-antenna systems.

Ray tracing has been used to obtain impulse response profiles at different locations in a building where extensive wideband propagation measurements have been carried out. The software was developed at the Center for Wireless Information Network Studies (CWINS) at Worcester Polytechnic Institute, and is described in [Yan94b]. Use of ray tracing to generate the impulse responses is validated by obtaining channel impulse responses for a set of locations using both measurements and ray tracing, and comparing the resulting two sets of BER estimates. The channel profiles obtained through ray tracing are then used to compare the performance of different transmission techniques. Given a fixed bandwidth, the "noise floor" error rate of direct sequence spread spectrum (DSSS) with one-, two-, and four-tap RAKE receivers and frequency hopping spread spectrum (FHSS) with and without channel coding are plotted as a function of data rate. Similar results for multicarrier modulation (MCM) with and without channel coding are plotted as a function of the number of carriers, since in the case of MCM the data rate is not a function of the number of carriers.

The above systems are compared with systems employing decision feedback equalization (DFE) and sectored antenna (SA) selective diversity, for which performance results were previously reported [Yan94b]. The maximum achievable data rate for each system is obtained, given a reasonable outage requirement and no bandwidth restrictions. For a fixed bandwidth, minimum power requirements are also presented.

2. Method for Analysis

In order for code division multiple access to be successful, it requires global power control [Kav87]. As a result, most existing systems, as well as the 802.11 standard, specify some form of contention-based time division access with collision avoidance [Tuc91, IEEE94]. Therefore, this paper does not address CDMA, assuming that the channel is used by at most one transmitter at a time.

2.1 Channel Model

The most popular model for describing multipath channels is the so-called discrete multipath time-domain model. It was developed by Turin to describe propagation in the urban radio channel, and was later applied to the indoor radio channel [Kav87, Yan94b]. It describes the channel as a linear time-invariant filter whose impulse response is the sum of L paths with the *lth* path having amplitude β_l, delay τ_l, and phase φ_l;

$$h(t) = \sum_{l=0}^{L-1} \beta_l \cdot \delta(t - \tau_l) \cdot e^{j\phi_l}$$

This model also lends itself well to ray-tracing, which generates the gain, delay, and phase of the surviving rays. These can simply be plugged into the above equation to yield the channel impulse response. In this paper we draw β_l, and τ_l from ray tracing. During the simulations, path phases φ_l are treated a

0-7803-3002-1/95 $4.00 ©1995 IEEE

random variables uniformly distributed in [0,2π], simulating small-scale movements of the transmitter and/or receiver, or motion of objects close to either unit.

2.2 System Descriptions

We examine five transmission techniques in this paper: DSSS, FHSS, MCM, DFE, and SA. QPSK modulation and coherent detection are assumed. At the transmitter, data is modulated onto the I and Q channels of a carrier. The signal is then passed through the spread spectrum or multicarrier modulator, and transmitted over the channel, where it is distorted by the channel multipath characteristics and AWGN. At the receiver, the signal is demodulated, despread (if applicable), and sampled at the time determined by the timing recovery circuit. The resulting decision variable is phase-compensated and used to determine the bits transmitted over the I and Q channels.

Spread Spectrum

The frequency hopping and direct sequence systems were described in detail in [Fal95]. In FHSS, the transmitter and receiver pulse-shaping filters, $g_r(t)$ and $g_t(t)$, are identical with a square root of raised cosine frequency response. The received signal is obtained by convolving the transmitter output with the channel impulse response and adding noise. This is then de-hopped and passed through the receiver's matched filter, yielding;

$$z(t|n) = \sum_i \sum_{l=0}^{L-1} b_i \cdot \beta_l \cdot g(t - iT - \tau_l) \cdot e^{j(2\pi f_n \tau_l + \phi_l + \theta_n)} + n_1(t)$$

where f_n is the nth carrier frequency, $\{b_i\}$ is the complex data sequence, θ_n is the phase offset between the FH modulator and demodulator, $n_1(t)$ is the front-end filter's response to AWGN, and $g(t)=g_r(t)*g_t(t)$ is the impulse response of a raised-cosine pulse shaping filter. Finally, z(t) is sampled and phase-compensated, yielding a decision variable conditioned on hop carrier n. The sampling time for a raised cosine pulse is obtained following the practical method derived in [Val87]. Perfect phase recovery was also assumed.

The DSSS system is assumed to have a spreading gain of N and chip period T_c , such that $T=N \cdot T_c$ is the bit period. The receiver filter is matched to the PN sequence, such that (without multipath), the cross-correlation of the transmitted signal and the periodic despreading signal has a peak of width T_c centered at zero delay. The despreader's output is therefore given by

$$z(t) = \sum_i \sum_{l=0}^{L-1} b_i \cdot \beta_l \cdot R_x(t - iT - \tau_l) \cdot e^{j\phi_l} + n_1(t)$$

where $R_x(\tau)$ is the cross-correlation of the PN sequence. The RAKE receiver used in the direct sequence system samples z(t) at the highest peaks, which are detected using a sliding window. It then phase-compensates the complex sample to yield the decision variable.

Multicarrier Modulation

The multicarrier system is shown in figure 1. Since a raised cosine pulse is assumed, error probability expressions -- again conditioned on carrier number n -- are similar to those for frequency hopping. However, depending on the frequency separation between carriers, interference from adjacent carriers may also need to be taken into account. If the total system bandwidth and number of carriers are fixed, increasing the distance between carriers will reduce the amount of interference from adjacent carriers, at the expense of data rate. Defining the time-bandwidth product as the product of symbol period T and frequency separation $\Delta\omega$, a time-bandwidth product of 1.5 was found to provide sufficient separation between carriers for a raised-cosine rolloff factor of 0.5. This was used throughout the simulations cited in this paper. The carriers are assumed to be equally spaced with the nth carrier given by $\omega_n = \omega_0 + (\Delta\omega)n$. Given reasonable pulse shaping filters, every carrier will only be interfered with by its two adjacent neighbors. The received signal on the nth carrier can therefore be written as

$$z(t|n) = \left\{ \sum_i \sum_{m=-1}^{1} b_{in} \cdot g_m(t - iT) \right\} * h(t) + n_1(t)$$

where

$$g_m(t) \equiv \int_{-\infty}^{\infty} g_t(\tau) \cdot e^{j(\Delta\omega)m\tau} \cdot g_r(t-\tau) \cdot d\tau$$

and b_{in} is the information bit transmitted on carrier n during the ith symbol interval. Exact expressions for $g_{+1}(t)$ and $g_{-1}(t)$ for a raised cosine pulse can be found in [Yan94a]; $g_0(t)$ is equivalent to g(t) in the frequency hopping system described above.

DFE and SA Systems

Performance results for decision-feedback equalizer and sectored antenna systems at this location were first reported in [Yan94b]. In the case of DFE modems, the overall sampled impulse response after equalization is used for z(t) [Pah95].

When sectored antennas are used, the channel impulse response for each antenna sector is modified to take into account the direction of arrival of each path. This analysis assumed that the receiver is equipped with a six-sector directional antenna whose polarizations are vertical. The ith antenna pattern is defined by the function

$$g_i(\psi) = \begin{cases} \dfrac{\sin\left(\dfrac{2.78 \cdot (\psi - \pi i/3)}{\Phi}\right)}{\dfrac{2.78 \cdot (\psi - \pi i/3)}{\Phi}} & \text{if } \dfrac{\pi i}{3} - \dfrac{\Phi}{2} \le \psi < \dfrac{\pi i}{3} + \dfrac{\Phi}{2} \\ a_0 & \text{otherwise} \end{cases}$$

where $g_i(\psi)$ is the normalized power gain for a ray arriving from angle ψ, and Φ is the antenna's 3dB beam width, which is set to $\pi/3$, resulting in a six-sector antenna. The pattern for one sector of this antenna is depicted in figure 2. The channel impulse response for the ith sidelobe is therefore given by

$$h_i(t) = \sum_{l=0}^{L-1} \beta_l \cdot \delta(t - \tau_l) \cdot e^{j2\pi\phi_l} \cdot g_i(\psi_l)$$

where ψ_l is the angle of arrival of the lth path.

2.3 Error Rate Analysis

Since QPSK modulation with coherent detection is assumed, error probability for the I and Q channels can be computed separately, and combined to arrive at a symbol error rate. The

same equations used for spread spectrum in [Fal95] are repeated for MCM, DFE, and SA systems. The receiver's front-end noise was computed following the derivation in [Lee89]; at an operating temperature of 290°K, thermal noise will be -174 dBm/Hz. In the case of direct sequence spread spectrum, the bandwidth of the front-end filter is 25 MHz, resulting in noise variance of about -100 dBm. In frequency hopping and multicarrier modulation, the front-end filter's bandwidth is dependent on the data rate, resulting in a higher noise variance at higher data rates (lower number of carriers).

In this paper we also study the effect of Reed-Solomon coding, when used in conjunction with frequency hopping or multicarrier modulation. If the encoder is an (n, k) coder defined over $G(2^m)$, it is capable of correcting up to (n-k)/2 errors [Pah95]. The number of bits per channel symbol is set equal to the number of carriers, and each bit of the resulting codeword is transmitted via a different carrier. The I and Q channels also carry bits from different codewords. The probability of codeword error is equal to the probability of having more than t bits in error. In this study, since the ray tracing program predicted the error probability of each channel separately, it was possible to use a more advanced technique to arrive at more accurate results. As described previously [Fal95], we follow the procedure presented in Appendix A of [Pur89]. We also assume that if a codeword is received in error, half of the decoded information bits will be in error.

2.4 Validation of Ray Tracing Method

From the perspective of system design -- and deployment -- the requirement is that impulse responses generated via ray tracing and those obtained from wideband measurements result in similar performance estimates for the transmission techniques under study. In [Fal95], channel impulse responses obtained from measurements and ray tracing were used to obtain error and outage probabilities for the same set of transmitter/receiver locations. It was shown that similar performance results are obtained from either set of impulse responses.

3. Results & Discussion

It is often desirable to view a data channel as on/off, where outage is defined as the bit error rate exceeding a certain threshold [Yan94b]. Outage probability can then be defined as the percent of time that a given location is in outage or the percent of locations that are in outage at a given time. The former is often used to describe time-varying channels such as urban mobile, while the latter is used to describe fixed installations such as indoor wireless LANs. In this study, an outage threshold of 10^{-5} was chosen. In this building, 100 mW of transmitted power (100 mW per carrier in the case of multicarrier systems) was found to eliminate the effects of additive noise for all three modulation techniques [Fal95]. It was therefore chosen as the noise floor power level.

3.1 Spread Spectrum

When combined with a RAKE receiver [Pah95], direct sequence spread spectrum provides sufficient resolution to allow individual paths to be extracted from the received signal, providing a form of time diversity. Frequency hopping spread spectrum, on the other hand, takes advantage of the fact that different portions of the spectrum tend to fade independently. Significant improvements can be achieved with a small reduction in data rate through the use of channel coding and interleaving, as described in the previous section.

Assuming QPSK modulation in a fixed bandwidth of 25 MHz, processing gains of 7, 15, 31, and 63 result in uncoded data rates of 7.1, 3.3, 1.6, and 0.79 MBPS, respectively. When channel coding is used, Reed-Solomon codes of (7,5), (15,11), (31,23), and (63,45) are used, so that in all cases the reduction in data rate is approximately a factor of 5/7. The resulting data rates are 5.1, 2.4, 1.2, and 0.57 MBPS for the FHSS system.

Figure 3 is a plot of outage probability vs. data rate for frequency hopping spread spectrum with and without Reed-Solomon coding and direct sequence spread spectrum with 1-, 2-, and 4-tap RAKE receivers employing maximal ratio combining. It can be seen that with a four-tap RAKE receiver, DSSS performs better than FHSS without coding. However, when coding is added to frequency hopping spread spectrum, its performance improves significantly; the error rate falls to practically zero with only 15 carriers.

3.2 Multicarrier Modulation

Using multicarrier modulation with a time-bandwidth product of 1.5, a system bandwidth of 25 MHz, and QPSK modulation resulted in a data rate of 33.3 MBPS. With coding, the data rate was reduced to 24 MBPS. Figure 4 shows the outage rate of multicarrier systems with and without channel coding, as a function of number of carriers (since the data rate was essentially constant).

Comparing these results with those of the previous section, it is obvious that in a bandlimited system that does not implement code division multiple access, for a given bit error rate, multicarrier modulation allows a higher data rate than either form of spread spectrum modulation. Furthermore, since it is obvious from figure 4 that the outage probability can be reduced by increasing the number of carriers, multicarrier modulation offers the potential of lowering the outage probability without a corresponding reduction in the data rate.

3.3 A Comparison Among Transmission Techniques

Table II of [Yan94b] presents the maximum data rates that can be achieved with DFE, SA, and DFE/SA systems, given an outage probability of .01 and assuming unlimited available bandwidth. Since these results were for BPSK modulation, the data rates were doubled to reflect the increased data rate achievable with QPSK modulation and perfect phase recovery. These numbers assumed no limit on the available bandwidth. Therefore, comparable results were obtained for the spread spectrum systems by repeating the simulations at different system bandwidths with the processing gain fixed. The results have been summarized in figure 5. Results for multicarrier modulation have not been presented, because (given no bandwidth limitations) the data rate of multicarrier systems is

infinite; the restriction in this case is the complexity of the system. To have outage rates of .01 or less, spread spectrum appears to only allow data rates of between 1 and 10 MBPS, even with no limits on the available bandwidth.

Based on the above discussion, it may appear that spread spectrum modulation is not a suitable transmission technique for wireless data networks. However, bandwidth efficiency is only one side of the equation; the processing gain that spread spectrum provides can serve to increase the fade margin, reducing the transmitter's power requirement. This could be an important consideration if the wireless network is being used to connect portable, battery-operated computers. Using the same outage criterion as above, the minimum power requirement of spread spectrum modulation was compared to that of MCM, DFE, and sectored antenna systems. Figure 6 shows the minimum power required to achieve an outage rate of .01 for DSSS with 4 taps, as well as FHSS and MCM with and without Reed-Solomon coding. Also presented are the power requirements to achieve the same outage probability using DFE, SA, and DFE/SA systems. A total system bandwidth of 10 MHz is assumed. According to this figure, spread spectrum can add between 30 and 35 dB to the fade margin. Furthermore, equalization itself is a power-intensive operation, a significant factor for portable, battery-operated computers. On the other hand, it can be expected that wireless networks that serve mostly portable users will operate at lower power levels with much smaller cells -- especially if significant processing gain is available. This will result in better frequency reuse, partially canceling the bandwidth inefficiency of spread spectrum modulation.

The power savings possible with spread spectrum modulation can only be achieved at the expense of data rate. On the other hand, multicarrier modulation can provide an improvement of about 20-25 dB, with only a small reduction in the data rate. As a result, in systems where both bandwidth efficiency and power consumption are important, multicarrier modulation can provide the best tradeoff.

4. Summary and Conclusions

Different transmission techniques have been presented, and compared using channel impulse responses generated by a ray tracing algorithm. Outage probability was plotted as a function of data rate for spread spectrum systems with different levels of system complexity and as a function of number of carriers for multicarrier modulation. These were compared with DFE, SA, and DFE/SA systems.

It was shown that spread spectrum is not an efficient way of combating multipath fading in an indoor environment; the loss in bandwidth efficiency is too high in a "large" LAN environment where throughput is a critical factor. On the other hand, in networks where users have battery-operated portable computers, due to smaller cell size and better frequency reuse, bandwidth efficiency requirements may not be as strict, making spread spectrum modulation more attractive due to its processing gain (which further reduces the power requirements). If both bandwidth efficiency and power consumption are important, multicarrier modulation appears to present the best tradeoff.

References

[Bou94] B. Bourin, "HIPERLAN - Markets and Applications Standardisation Issues", IEEE Int'l. Conf. on Personal, Indoor, and Mobile Radio Communications, Hague, Netherlands, Pp. 863-868, Sept. 1994.

[Cha93] M. Chase, K. Pahlavan, "Performance of DS-CDMA Over Measured Indoor Radio Channels Using Random Orthogonal Codes", IEEE Trans. on Vehicular Technology, Vol. 42, Pp. 617-624, Nov. 1993.

[Fal95] A. Falsafi, K. Pahlavan, "A Comparison Between the Performance of FHSS and DSSS for Wireless LANs Using a 3D Ray Tracing Program", IEEE Vehicular Technology Conference, Chicago, IL, July 1995.

[IEEE94] IEEE Std. 802.11-93/20b3, "Wireless LAN Medium Access Control (MAC) and Physical Layer (PHY) Specifications", draft standard, September 1994.

[Kav87] M. Kavehrad, B. Ramamurthi, "Direct Sequence Spread Spectrum with DPSK Modulation and Diversity for Indoor Wireless Communications", IEEE Transactions on Communications, Vol. 35, Pp. 224-236, February 1987.

[Lee89] W. C. Y. Lee, Mobile Cellular Telecomm. Systems, New York, McGraw-Hill, 1989.

[Pah95] K. Pahlavan, A. Levesque, Wireless Information Networks, John Wiley, 1995.

[Pur89] M. Pursley, S. Sandberg, "Variable-rate Coding for Meteor-burst Communications", IEEE Transactions on Communications, Vol. 37, Pp. 1105-1112, Nov. 1989

[Tuc91] B. Tuch, "An ISM Band Spread Spectrum Locan Area Network: WaveLAN", IEEE Workshop on Wireless Local Area Networks, Worcester, MA, Pp. 103-111, May 1991.

[Val87] R. Valenzuela, "Performance of Quadrature Amplitude Modulation for Indoor Radio Communications", IEEE Trans. on Comm., Vol. 35, Pp. 1236-1238, Nov. 1987.

[Yan94a] G. Yang, K. Pahlavan, "Performance Analysis of Multicarrier Modems in Office Environment Using 3D Ray Tracing", IEEE GLOBECOM '94 San Francisco, CA, Pp. 42-46, November 1994.

[Yan94b] G. Yang, K. Pahlavan, T. Holt, "Sector Antenna and DFE Modems for High Speed Indoor Radio Communications", IEEE Trans. on Vehicular Technology, Vol. 43, Pp. 925-933, Nov. 1994.

Fig. 1 - Multicarrier Modulation System

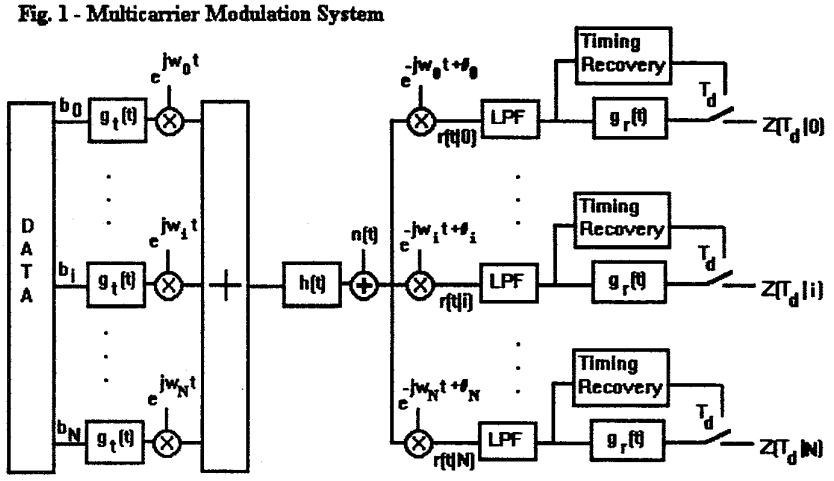

Fig. 2 - Antenna pattern for one sector of six-sector antenna.

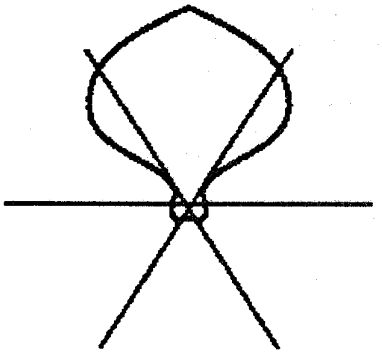

Fig. 3 - P(outage) for Spread Spectrum, 25MHz, 100mW

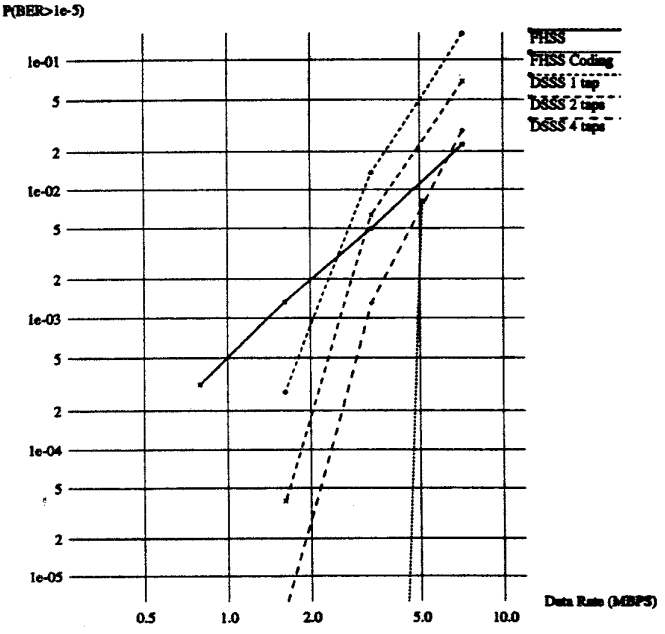

Fig. 4 - P(outage) for Multicarrier Modulation, 25MHz, 100mW

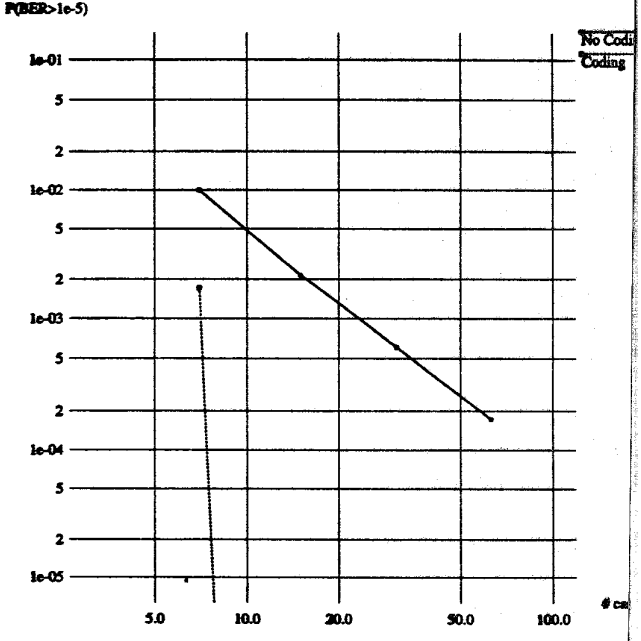

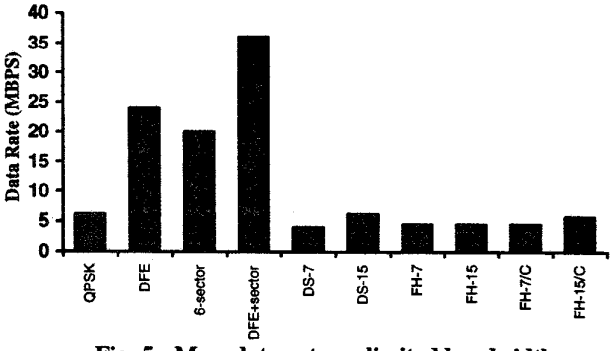

Fig. 5 - Max. data rate, unlimited bandwidth

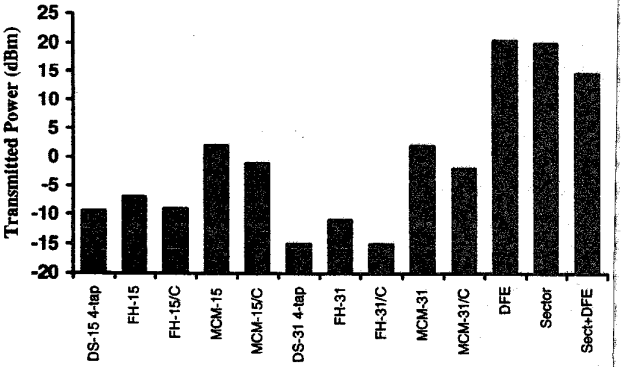

Fig. 6 - Min. power, 10MHz Total Bandwidth